

Research Article

Influence of damage state threshold variability on the seismic vulnerability analysis of masonry aqueducts

Ali Yesilyurt a,* (D)

^a Department of Earthquake Engineering, Disaster Management Institute, İstanbul Technical University, 34469 İstanbul, Türkiye

ABSTRACT

The accuracy of fragility curves, a key outcome of seismic vulnerability studies, directly influences rational seismic risk assessments. In this study, analytical-based fragility curves for a masonry aqueduct were derived using tested earthquake-based Intensity Measure (IM) parameters and various threshold limit values for specific damage states, as commonly used in the literature. The Maximum Intensity Damage Ratio (MIDR) thresholds for specific damage states proposed by FEMA 356, GERMHS, and ASCE 41-13 standards were considered. Additionally, damage state thresholds were determined through a capacity curve obtained via nonlinear static analysis and empirical relationships found in the literature. The effect of damage thresholds on the Probability of Exceedance (PoE) values for a specific damage state was analyzed using the reference MIDR values determined in this study. Based on earthquake ground motion records, PoE values corresponding to different damage states were evaluated separately for each IM parameter. The results demonstrate that the damage threshold value significantly impacts the developed fragility curves. Therefore, when developing fragility curves for the seismic risk assessment of masonry structures, it is crucial to analyze and determine the appropriate threshold levels for each structure individually, rather than directly applying the threshold values used in the literature.

ARTICLE INFO

Article history:

Received – May 2, 2025 Revision requested – June 2, 2025 Revision received – June 10, 2025 Accepted – June 20, 2025

Keywords:

Masonry aqueduct Intensity measure Cloud Analysis Drift ratio Fragility curve



This is an open access article distributed under the CC BY licence. © 2025 by the Author.

Citation: Yesilyurt A (2025). Influence of damage state threshold variability on the seismic vulnerability analysis of masonry aqueducts. *Challenge Journal of Structural Mechanics*, 11(3), 137–148.

1. Introduction

Aqueducts are significant engineering structures built to transport water from natural sources to settlements by crossing valleys, rivers, and various natural or artificial obstacles. These structures, tangible examples of the masonry design approach that developed particularly from ancient times onward, reflect past civilizations' technical knowledge and aesthetic sensibilities. Numerous surviving masonry aqueducts draw attention today not only for their historical significance but also for their architectural and cultural heritage value (Balcan et al. 2024). Although modern infrastructure systems are widely used today and contemporary water conveyance structures are being constructed, numerous aqueducts

belonging to different cultures remain standing within the borders of present-day Türkiye (Fig. 1).

Despite having lost their original function, these structures are preserved as significant elements of cultural heritage due to their architectural characteristics and historical value (Gonen et al. 2021). Preserving these engineering marvels and passing them on to future generations is of great importance. However, there are relatively few comprehensive studies that assess the seismic vulnerability and risk of such historic structures (Dogangun and Sezen 2012). In general, historic masonry aqueducts are classified into sub-categories based on their construction techniques, material properties, and geometric configurations. Seismic vulnerability and risk assessments are conducted for each subcategory

separately (Çakır 2021; Ercan et al. 2015). Seismic vulnerability and risk assessment studies are of crucial importance, with the objective being the quantification of potential damage and losses caused by earthquakes. The capacity to predict accurately the losses that a given type of structure may encounter post-earthquake is a critical reference, as it enables the effective planning of both pre-earthquake preparedness and post-earthquake action and rehabilitation processes (Cattari et al. 2022; Yücemen and Yılmaz 2015; Işık et al. 2020). Fragility curves are a valuable tool that provides the probability of exceeding (PoE) a particular damage state for a given

seismic intensity measure parameter value. A review of the existing literature shows that fragility curves are extensively utilized in seismic risk analysis (Yesilyurt et al. 2024; Rota et al. 2010; Yesilyurt et al. 2021a). It is known that the extant literature on seismic risk studies of historical masonry structures is more limited compared to traditional residential buildings, industrial structures, and steel constructions (Gkournelos et al. 2022; Alpaslan and Karaca 2020; Lagomarsino and Cattari 2015). Moreover, the scarcity of literature addressing the seismic fragility functions specific to masonry aqueducts is particularly pronounced.

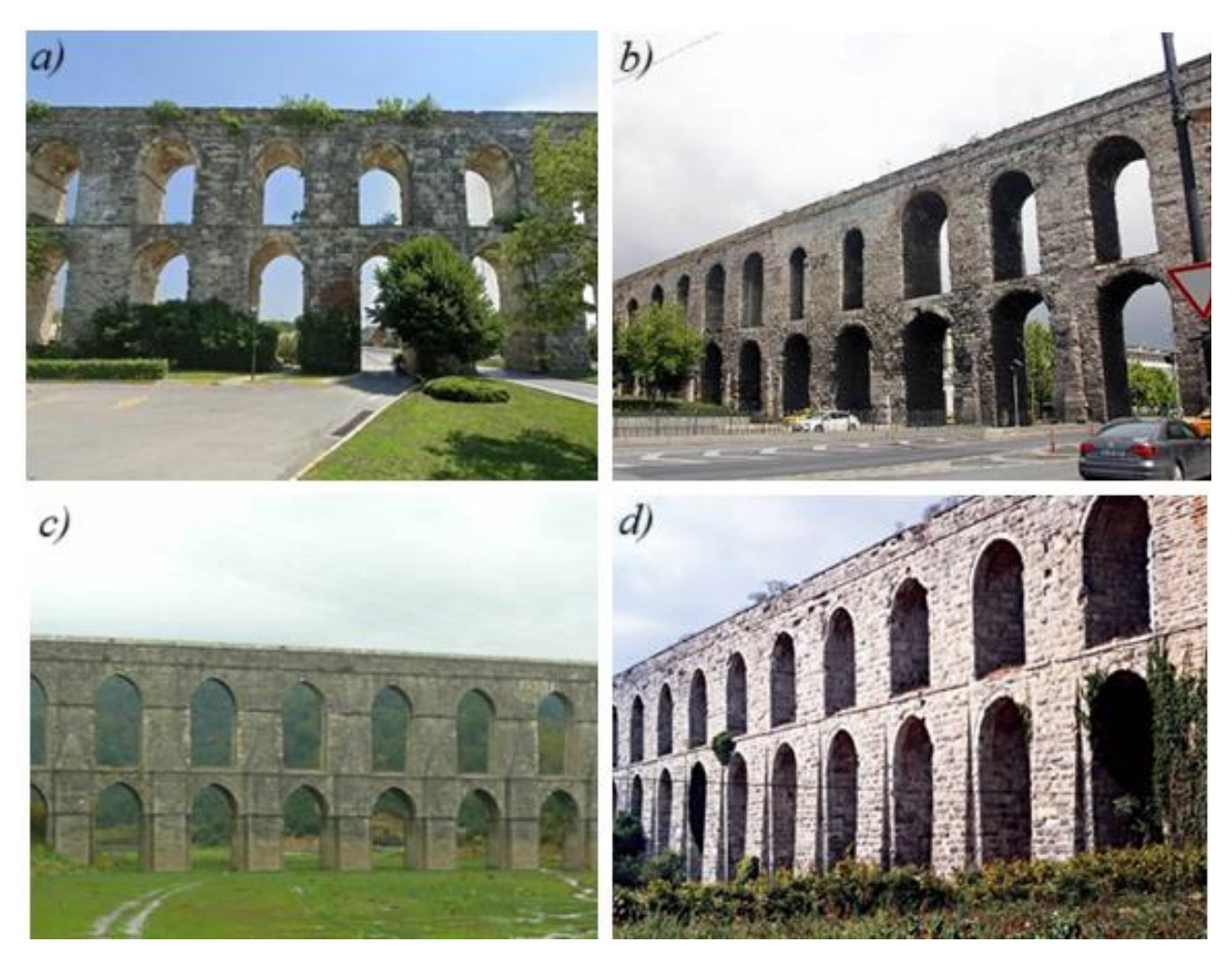


Fig. 1. Examples of masonry aqueducts located in Türkiye: a) Uzun Aqueduct; b) Bozdogan (Valens) Aqueduct; c) Güzelce Aqueduct; d) Kırkçeşme Aqueduct.

Du et al. (2023) derived fragility curves based on peak ground acceleration (*PGA*) for a sample aqueduct in south-west China. The effects of both mainshock and aftershock ground motion sequences were considered. The Incremental Dynamic Analysis (IDA) method was applied. The impact of aftershocks on seismic risk was examined through the fragility surface. Liu et al. (2025) conducted a seismic vulnerability analysis of a threespan simply supported aqueduct in China. The probability of damage under seismic loading was analyzed through the implementation of probability density functions. In the study by Zhang et al. (2022), the seismic response of high-span aqueduct structures was in-

vestigated under Near-Far field ground motions, with fragility curves developed as a function of *PGA*. A comparative assessment of *PoE* at specific intensity measure levels revealed that aqueduct structures are more vulnerable to damage under near-fault ground motions. In a similar study, Zheng et al. (2023) examined the effects of aftershocks on structural damage. The IDA method was employed, and seven main aftershock sequences were considered. Fragility curves were proposed for four different damage states as a function of *PGA*. For specific *PGA* values, the damage-increasing effect of aftershocks was assessed based on the exceedance probability.

Xu et al. (2021) developed fragility curves for a largescale aqueduct structure using IDA and the Multiple Stripe Analysis (MSA) method. The study considered four distinct damage states, and the fragility curves were derived as a function of spectral acceleration (Sa). Du et al. (2024a) presented fragility curves for a typical threespan aqueduct structure by considering both single and compound intensity measures. Moreover, the study provided quantitative recommendation values regarding record-to-record variability, design parameters, performance index values, and limit states. Yesilyurt (2025) proposed the earthquake and structure-based optimal intensity measure (IM) parameters for quantifying the seismic risk of a typical Roman masonry aqueduct. The study considered 29 IMs, and fragility curves were derived based on the identified optimal IMs and various damage parameters. Similarly, the suitability of IMs for modern aqueduct structures was examined through the utilization of near-field non-pulse, near-field pulse, and far-field sets of ground motion records. The influence of these ground motion sets on *PoEs* was also analyzed for the selected optimal IMs (Du et al. 2024b).

Ma et al. (2022) developed component-based fragility curves for a three-span aqueduct with an equidistant simply supported beam. The general product of conditional marginal method is performed. The study incorporated both structural and ground motion uncertainties to develop fragility curves. Similarly, Cheng et al. (2020) developed component-based fragility curves for a typical aqueduct structure.

In addition to the aforementioned studies, the maximum inter-story drift ratio (*MIDR*) is frequently utilized as a damage parameter in the risk assessment of historic masonry structures (Korkmaz et al. 2018; Vanin et al. 2017; FEMA 274 1997). Furthermore, various standards provide threshold values for different damage states based on the *MIDR* parameter. The primary objective of this study is to develop analytically based fragility curves for aqueduct structures using these predefined threshold values. Subsequently, the study aims to investigate the impact of these thresholds on seismic vulnerability assessment.

To this end, a finite element model of a typical masonry aqueduct was constructed. Response spectrum analyses were then performed using the cloud analysis method on a set of 479 ground motion records. The dispersion between the selected *IMs* and the *MIDR* damage parameter was obtained. Based on these intensity and damage measure relationships, fragility curves were derived separately for different thresholds. Furthermore, the *PoE* values corresponding to different damage states were comparatively analyzed for selected earthquake ground motion records.

2. Seismic Vulnerability Analysis

An examination of the seismic-tectonic setting of Türkiye reveals that the Arabian plate, located to the south, is moving northwards and colliding with the Eurasian plate, resulting in significant compression in the eastern Anatolian region. As a result of this plate interaction, the Anatolian plate is being pushed westward, mainly by the

North Anatolian Fault Zone (NAFZ) and the East Anatolian Fault Zone (EAFZ) (Erdik et al. 1985).

Among the major destructive earthquakes that have occurred in Türkiye over the past 30 years are the 17 August 1999 Mw 7.4 Kocaeli, 12 November 1999 Mw 7.2 Düzce, 3 February 2002 Mw 6.4 Afyon, 1 May 2003 Mw 6.4 Bingöl, 23 October 2011 Mw 7.2 Van, 24 January 2020 Elazığ, 30 October 2020 Mw 6.9 Samos (İzmir), and 23 November 2022 Mw 5.9 Düzce earthquakes. In the recent past, a sequence of earthquakes that struck on February 6, 2023, centered in Kahramanmaraş, caused unprecedented destruction and loss of life, marking one of the most powerful and impactful seismic events in Türkiye's history. The epicentres of the two destructive earthquakes were located in the districts of Pazarcık and Elbistan, with focal depths measured at 8.6 km and 7.0 km, respectively. The rupture occurred along the northern segment of the East Anatolian Fault and severely affected several provinces (AFAD 2023). Furthermore, numerous unique historic masonry structures were destroyed during these events (Kocaman 2023; Kocaman et al. 2024; Erkek and Yetkin 2023). Seismic vulnerability and risk analyses are vital studies in reducing casualties following earthquakes. The recurrence of similar loss of life and property after earthquakes has increased interest in such studies (Alparslan et al. 2017; Cosgun and Mangir 2018). In parallel with technological advancements, there has been an increase in the number of seismic vulnerability and risk analyses studies, which are becoming more comprehensive and effective.

In the context of seismic vulnerability and risk mitigation studies, the RADIUS project, HAZUS (Multi-hazard Loss Estimation Methodology), PBEE-PBEE methodology, DBLA (the Displacement-Based Loss Assessment), ESPREME, GEM (Global Earthquake Model), RADIUS (Risk Assessment Tools for Diagnosis of Urban Areas against Seismic Disasters), SHARE (Seismic Hazard Harmonization in Europe), the SESAME project, NGA (Next Generation Attenuation) project, LESSLOSS, RISK-UE, The World Bank's CAPRA, SYNER-G, and NERA projects provide insightful guidance. Fragility curves are widely preferred in risk assessment calculations because of the convenience they provide (Yılmaz et al. 2018). These curves can be developed using empirical, analytical, hybrid, and expert judgement methods (Yesilyurt et al. 2021b). In this study, the analytical method has been considered, and the main components can be outlined as follows: numerical modelling, Compilation of an Earthquake Ground Motion Set, definition of damage and intensity measure parameters, structural analysis, damage analysis, and statistical procedures.

2.1. Description of the modelling and non-linear static analysis

Three-dimensional finite element modeling (FEM) is widely recognized as a reliable and effective approach for the seismic performance assessment of historical masonry structures. In this study, the finite element model of the investigated segment of the masonry aqueduct was developed using ANSYS Workbench. A visual of the 3D structural model considered in the analysis is presented in Fig. 2.

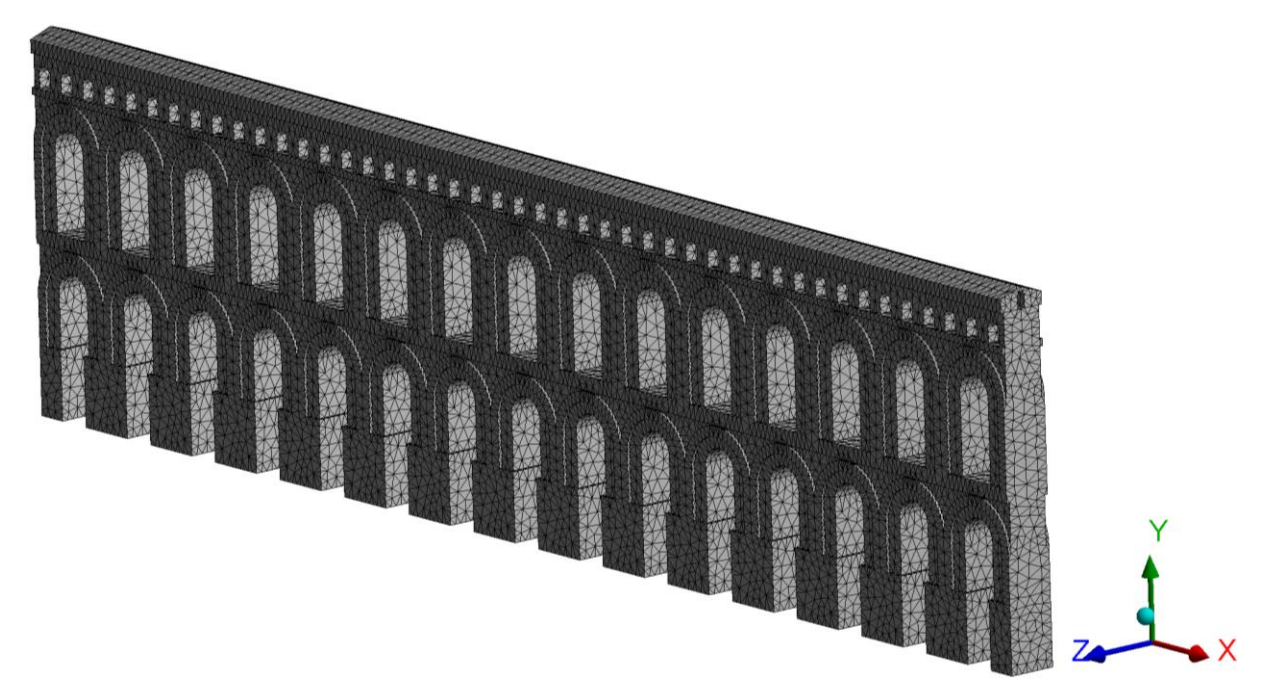


Fig. 2. Three-dimensional finite element model of the masonry aqueduct.

The 3D finite element model contained 261,619 nodes and 151,406 elements, utilizing a 20-node solid element with 3 degrees of freedom per node. Research on the most accurate modeling approaches for masonry structures continues to be a subject of advanced engineering studies. In this study, to improve computational efficiency in structural modeling, the aqueduct was treated as a homogeneous composite material, and the macro modeling approach was adopted, in which the masonry units and mortar are represented as a single equivalent material (Drougkas 2022). The aqueduct was modeled with fixed boundary conditions applied along its base and at its end supports. To accurately capture the nonlinear mechanical behavior of the masonry material, the Drucker-Prager yield criterion, which is considered suitable for materials with low tensile and high compressive strength, was employed (Drucker and Prager 1952).

As previously discussed, the primary objective of this study is to investigate the influence of different damage thresholds on the seismic vulnerability of the structure. The material properties used in the finite element modelling were determined based on previous studies in the literature and generally accepted engineering assumptions. The mechanical properties of the stone material considered were defined as Young's modulus 8729.6 MPa, Poisson's ratio 0.1238, bulk modulus 3.867×10⁹ Pa, and shear modulus 3.88×10⁹ Pa. In addition, the main parameters of the bilinear isotropic hardening model, yield strength and the tangent modulus, were considered as 3.2 MPa and 144 MPa, respectively.

A modal analysis was carried out to evaluate the seismic behavior and to examine the dynamic characteristics of the aqueduct. The first 30 vibration modes were considered to fully evaluate the dynamic response of the structure. This analysis identified the natural frequencies, periods, and mode shapes of the structure. The first six mode shapes and their corresponding frequency values are shown in Fig. 3.

In Fig. 3, the X, Y, and Z directions correspond to the in-plane, vertical, and out-of-plane directions of the structure, respectively, for the first six mode shapes. It is observed that the first mode of the aqueduct is in the out-of-plane (Z) direction, characterized by translational motion. This mode represents the most critical direction in the seismic performance of the structure. The out-of-plane response has been determined as a reference in the seismic vulnerability assessment. Therefore, in the subsequent cloud analysis, which will be detailed in the following sections, the structural response is primarily evaluated in the Z-direction, taking into account the out-of-plane behavior.

A non-linear static analysis was performed using an incremental-iterative procedure to evaluate the out-of-plane seismic performance of the structure based on the finite element model. The capacity curve calculated by the pushover analysis is shown in Fig. 4.

2.2. Definition of damage and intensity measure parameters

As previously stated, in seismic vulnerability studies, the Damage Measure (DM) parameter quantitatively defines the limit value of a specific damage state of a given structure. A review of studies conducted on masonry structures in the literature shows that the MIDR damage parameter is commonly utilized. Numerous studies, codes, and standards such as ASCE 41-13 (2013), FEMA 356 (2000), GERMHS (2017), have proposed threshold values corresponding to different damage states based on the MIDR damage parameter. When these studies are analyzed as a whole, it is observed that the thresholds proposed for a given damage state vary considerably. The objective of this study is to evaluate the influence of different threshold values on seismic vulnerability through fragility curves. In this context, initial damage (Damage Limitation) and expected partial collapse (Heavy Damage) have

been considered. The rationale behind this selection is related to the inherent characteristics of historic masonry structures, such as aqueducts, which exhibit limited nonlinear behavior and are prone to sudden brittle failure.

Furthermore, the yield and ultimate points on the capacity curve of the analyzed structure can be determined precisely. In this context, Table 1 presents the thresholds based on the MIDR parameter considered in this study.

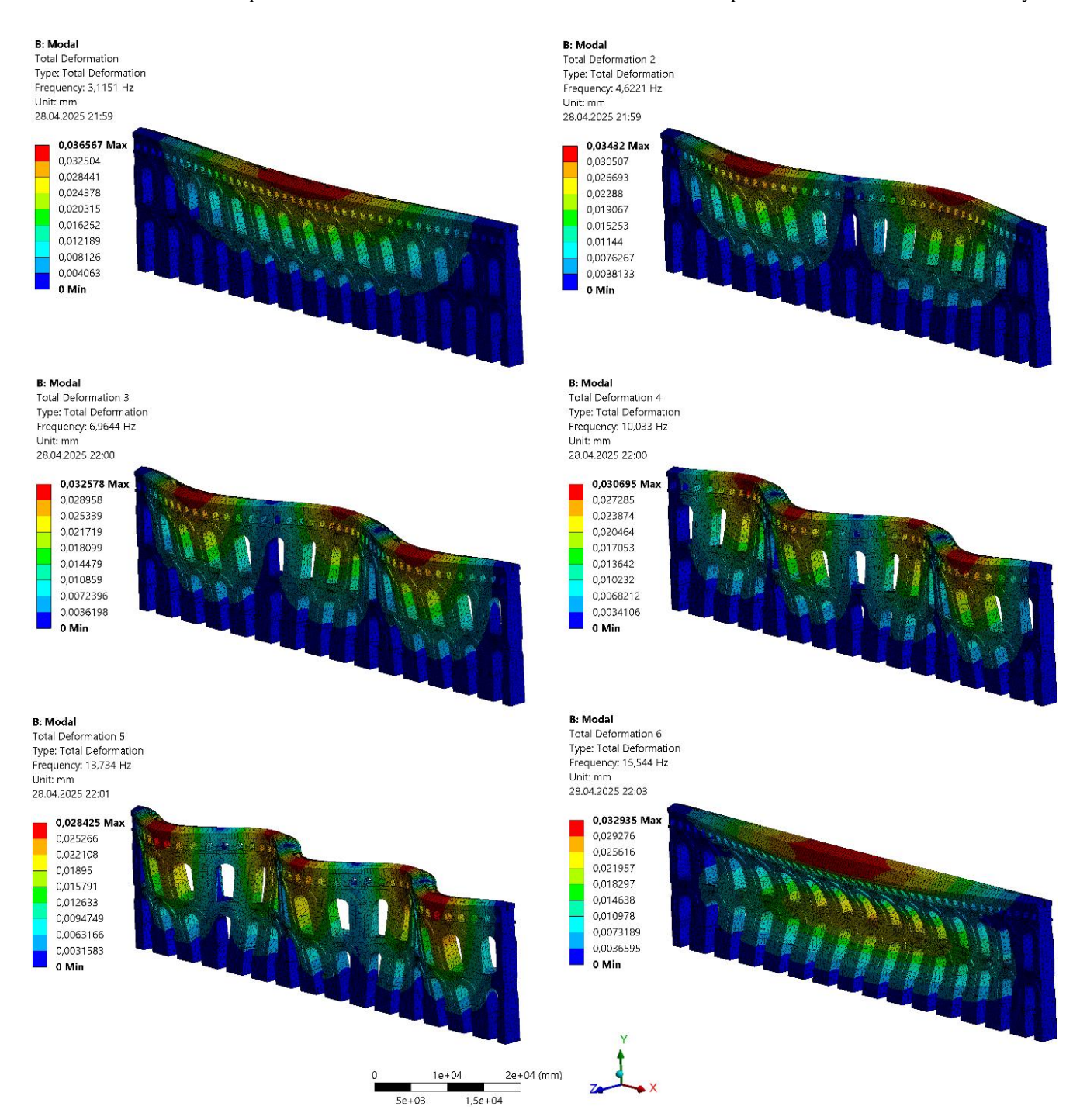


Fig. 3. The first six mode shapes and corresponding frequency values of the model.

Table 1. Various MIDR threshold values used as references for masonry structures.

Standards	Damage limitation (%)	Heavy damage (%)
FEMA 356 (2000)	0.10	0.40
GERMHS (2017)	0.30	0.70
ASCE 41-13 (2013)	0.10	0.75
Current study	0.18	0.53

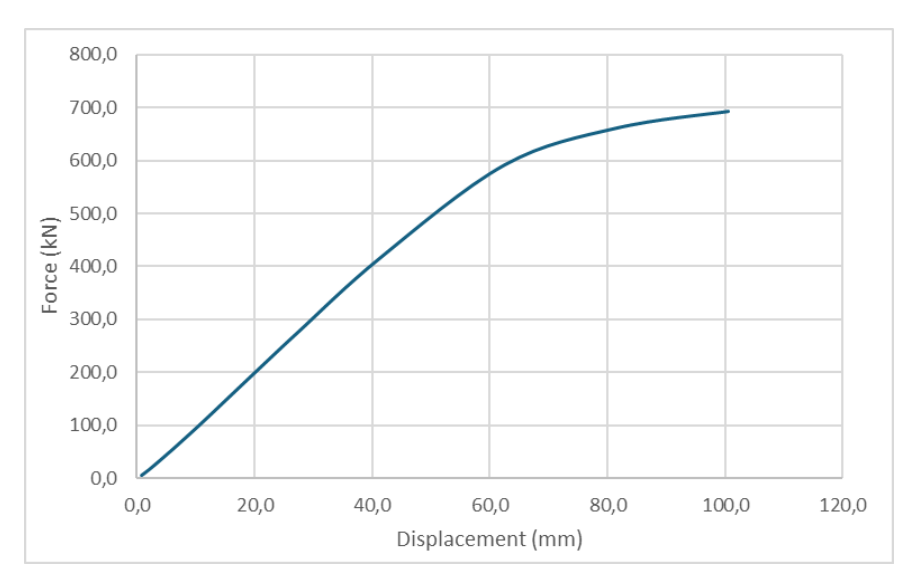


Fig. 4. Capacity curve of the aqueduct structure in the out-of-plane direction.

As can be seen in Table 1, in addition to the MIDR values presented in the existing standards, this study has provided different threshold values corresponding to structure-specific damage states. As demonstrated in numerous studies conducted by various researchers, the vield (dv) and ultimate (du) displacement values obtained from the capacity curve have been used as reference points to define different damage states (Lamego et al. 2017; Kappos et al. 2006; Vicente 2008; Lagomarsino and Giovinazzi 2006). In the relationship proposed by Kappos et al. (2006), 0.7 dy is suggested for Damage Limitation, while du is recommended for Heavy Damage. These threshold values have been calculated by utilizing the capacity curve depicted in Fig. 4 and the empirical relationships proposed by Kappos et al. (2006) as a reference.

The appropriateness of the IM parameters, which characterize ground motion and reflect the destructive potential of an earthquake, for a given class of structure directly impacts the accuracy of the derived fragility curves for that class. It is well known in the literature that the appropriate IMs vary depending on the structural typology. In this study, the earthquake-based IMs evaluated by Yesilyurt (2025) for their applicability in assessing the seismic vulnerability of aqueduct structures, namely Acceleration Spectrum Intensity (ASI), Arias Intensity (*Ia*), Characteristic Intensity (*Ic*), Sustained Maximum Acceleration (SMA), Effective Design Acceleration (EDA), and Peak Ground Acceleration (PGA) are considered. Accordingly, the analytically derived fragility curves are developed as functions of these IM parameters.

2.3. Seismic performance analysis method

The Cloud analysis method is particularly well-suited to vulnerability assessment of structures. In this method, the real unscaled ground motion records are utilized with a wide frequency range. This analysis approach can be adapted to various methodologies, including dynamic analysis, modal pushover analysis, and response spec-

trum analysis. The response spectrum analysis method is a widely employed technique in the relevant literature to evaluate the seismic performance and vulnerability of historical masonry structures. This is since it is both computationally efficient and practical (Akturk et al. 2025). The method has been employed in the analysis of finite element models of various masonry structures, including churches, mosques, arch bridges, and slender structures. The findings demonstrated a high level of consistency with post-earthquake field observations (Cakir et al. 2015; Ozdemir et al. 2017; Cakir et al. 2016; Cakir 2022).

In this study, the response spectrum method was adopted for performing structural analyses. In methods such as IDA, which involve a scaling process, the frequency content of the ground motion records remains unchanged. In contrast, the cloud analysis approach utilizes unscaled original ground motion records. This enables the consideration of a broader range of intensity and frequency characteristics, rather than being limited to the seismicity of a specific region.

The main challenge of this method lies in the necessity to include a large number of ground motion records to ensure that the selected set can adequately capture the overall structural response, ranging from slight damage to heavy damage. To this end, the ordinary earthquake ground motion record set was considered. This set incorporated near-far fault effects and all rupture mechanisms. A total of 479 real processed ground motion records were selected from the Pacific Earthquake Engineering Research Center (PEER) Ground Motion Database for the structural analysis of the aqueduct. The distribution of the sites where the selected ground motion records were recorded, along with the relationship between earthquake magnitude and source-to-site distance for the generated earthquake set, is presented in Fig. 5. Response spectrum analyses were performed on 479 real, unscaled earthquake records. The scatter plots illustrating the relationship between the IM parameters ASI, Ic, Ia, SMA, EDA, and PGA, as defined in the previous section, and the MIDR damage parameter are shown in Fig. 6.

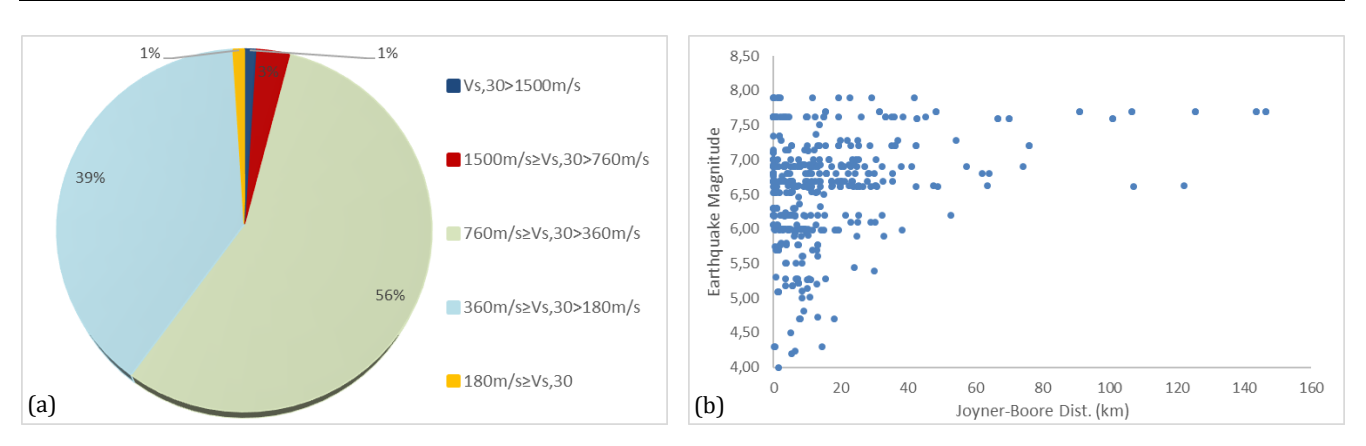


Fig. 5. Earthquake ground motion records: a) Site information at the locations of the stations; b) Magnitude-Distance relationship.

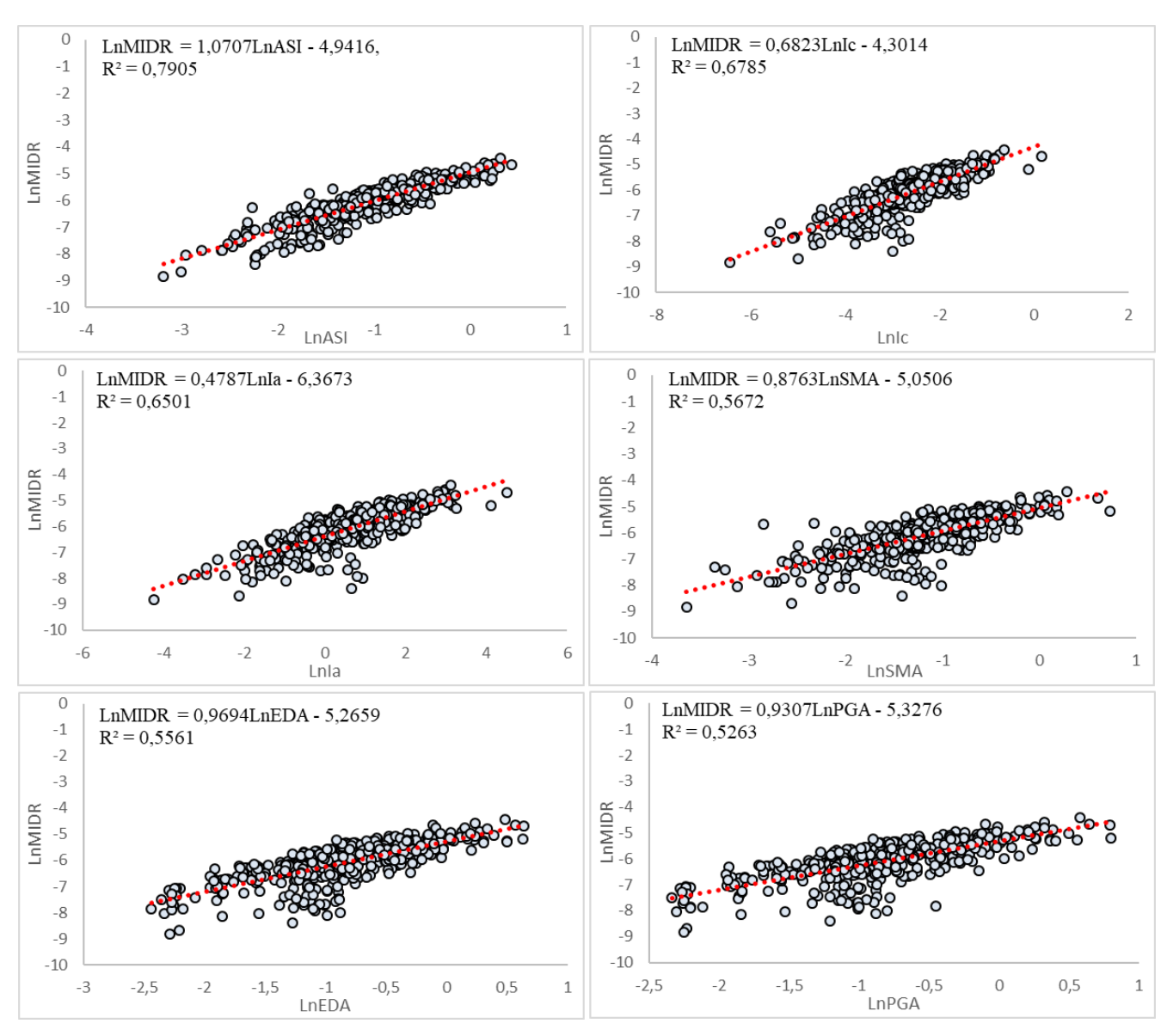


Fig. 6. *DM-IM* scatter plots computed using the cloud analysis method.

As shown in Fig. 6, *DM–IM* scatter plots were obtained for the aqueduct structure considered in this study using the *IM* parameters evaluated by Yesilyurt (2025) for their suitability. Among these, the *ASI* parameter exhibits a denser clustering of data points around the linear

regression line, clearly indicating that the standard deviation associated with this ASI-MIDR pair is lower compared to the others. Furthermore, the highest goodness of fitting (\mathbb{R}^2) and the regression slope (b) were also computed for the ASI parameter.

The main objective of this study is to examine the effect of different damage threshold levels on structural vulnerability. Therefore, fragility curves were developed for the six *IM* parameters shown in Fig. 6 using the threshold values given in Table 1.

2.4. Analytical-based fragility curve

As explained in the previous sections, fragility curves are functions that represent the *PoE* of a certain damage state for a given level of ground motion intensity measure. The procedure for deriving analytical-based fragility curves using the cloud analysis method consists of four main steps. First, *DM-IM* distributions are obtained for the set of earthquake ground motions considered in the study. These distributions illustrate the relationship between the seismic damage parameter and the selected intensity measure parameter. Second, the distribution of the damage parameter corresponding to each intensity level is analyzed, and the probability density function of the damage parameter is computed. In the next step, the damage measure variable is transformed into a log-normal distribution, and the cumulative distribution func-

tion of the log-normal variable is obtained. Based on the threshold values defined in Table 1, the probabilities of reaching or exceeding each damage state are discretely calculated by repeating the process for each intensity level. In the final step of the procedure, the obtained cumulative log-normal probability distribution is fitted to the most appropriate curve. Subsequently, fragility curves are constructed for each damage state, utilizing a two-parameter log-normal distribution, specifically the median (IM_{DS_i}) and logarithmic standard deviation (β_{DS_i}), according to Eq. (1).

$$P[\text{Damage} \ge DS_i | IM] = \Phi\left(\frac{\ln(IM) - \ln IM_{DS_i}}{\beta_{DS_i}}\right)$$
 (1)

In Eq. (1), ϕ denotes the standard cumulative normal distribution function, and IM represents ground motion intensity measure. In this study, fragility curves were derived separately for each IM parameter using the threshold values presented in Table 1. The fragility curves corresponding to the Damage Limitation state are presented in Fig. 7, while those corresponding to the Heavy Damage state are shown in Fig. 8.

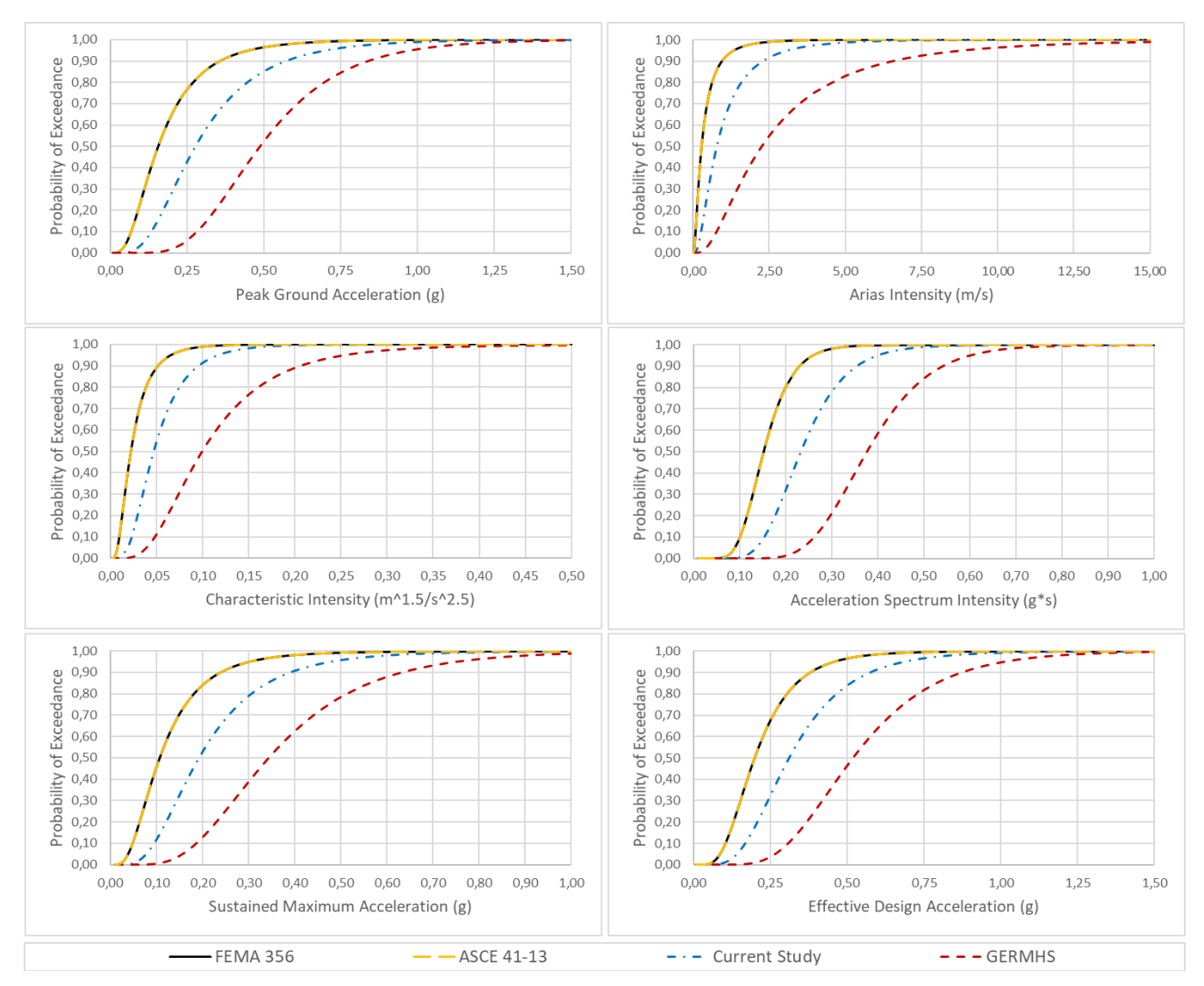


Fig. 7. Fragility curves derived for the Damage Limitation state, taking into account IMs and damage state threshold values.

The fragility curves presented in Figs. 7 and 8 illustrate the probabilistic relationship between seismic demand and the probability of exceeding the Damage Limitation and Heavy Damage state thresholds, emphasizing the impact of varying threshold values on seismic vulnerability.

Since the threshold values for the Damage Limitation state defined by FEMA 356 (2000) and ASCE 41-13 (2013) are identical, the fragility curves presented in Fig. 7 overlap. The fragility curves derived using the threshold values provided by these two standards yield the highest *PoEs* for a given *IM* value. In contrast, the lowest exceedance probabilities are computed using the threshold defined by GERMHS (2017). When the fragility

curves developed based on the threshold levels proposed in the current study are taken as reference, *PoE* values computed for a given *IM* value are found to be higher than those based on the GERMHS (2017) threshold, but lower than those obtained using the threshold values from the other two standards. Examining the fragility curves for the Damage Limitation state in Fig. 7, it is observed that for the *PGA IM* value of 0.25 g, the *PoE* was calculated as 0.765, 0.765, 0.425, and 0.057 for FEMA 356 (2000), ASCE 41-13 (2013), the current study, and GERMHS (2017), respectively. Similarly, for the SMA IM value of 0.30 g, these PoE values were determined to be 0.951, 0.951, 0.792, and 0.389, respectively.

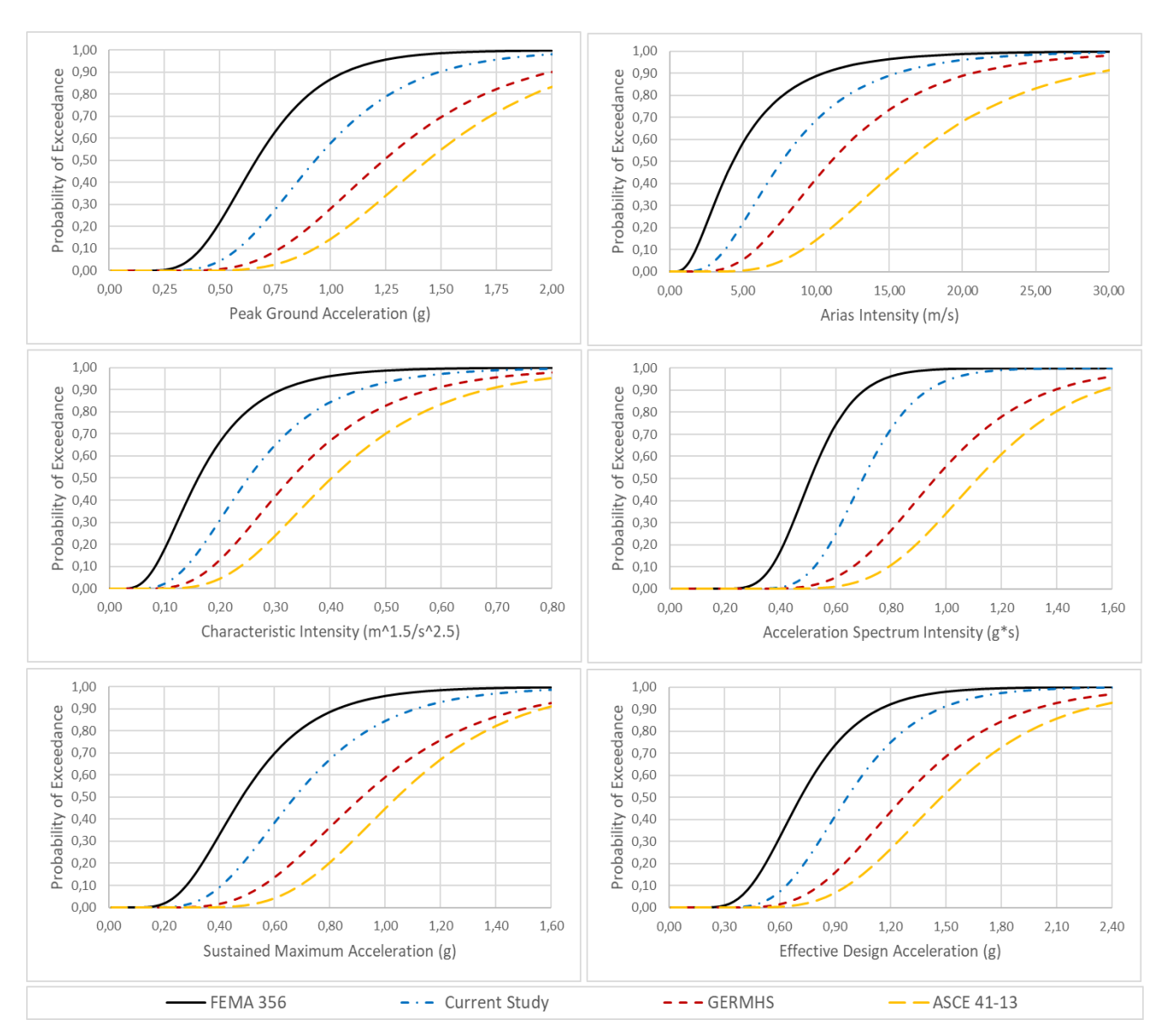


Fig. 8. Fragility curves developed for the Heavy Damage state, considering appropriate intensity measures and damage state threshold values.

In Fig. 8, the fragility curves developed for the Heavy Damage state indicate that, for a given *IM* level, the highest *PoE* is obtained using the FEMA 356 (2000) standard, while the lowest exceedance probability is ob-

served for the ASCE 41-13 (2013) standard. The fragility curves developed in the current study show *PoEs* that are higher than those of GERMHS (2017) and ASCE 41-13 (2013), but lower than those associated with

FEMA 356 (2000) for the same *IM* value. Fig. 8 shows the *PoE* values for the Heavy Damage state for the *EDA IM* parameter value of 1.2 g, which were calculated as 0.922, 0.748, 0.433, and 0.265 for FEMA 356 (2000), the current study, GERMHS (2017), and ASCE 41-13 (2013), respectively. Similarly, for the *AI* value of 10 m/s, the corresponding *PoE* values were computed as 0.887, 0.688, 0.423, and 0.144 for FEMA 356 (2000), the current study, GERMHS (2017), and ASCE 41-13 (2013), respectively.

To enable a more comprehensive assessment, the *PoE* values for the Damage Limitation state, computed using earthquake ground motion records RSN95 and RSN517, are presented in Fig. 9. Similarly, Fig. 10 illustrates the *PoE* values calculated for the Heavy Damage state using

ground motion records RSN143 and RSN1004.

As illustrated in Fig. 9, when the Current study is taken as a reference, the influence of damage threshold levels on the *PoE* varies depending on the earthquake record and the selected *IM*. For example, for a RSN95 record and *PGA*, the computed *PoE* values for the current study, FEMA 356 (2000), ASCE 41-13 (2013), and GERMHS (2017) are 0.6578, 0.893, 0.893, and 0.216, respectively. Similarly, the Heavy Damage state in Fig. 10, for RSN143 and *Ic*, the *PoE* values computed for the current study, FEMA 356 (2000), GERMHS (2017), and ASCE 41-13 (2013) are 0.745, 0.9268, 0.531, and 0.345, respectively. Similar assessments can also be conducted for other *IM* parameters that provide internally consistent *PoE* values.

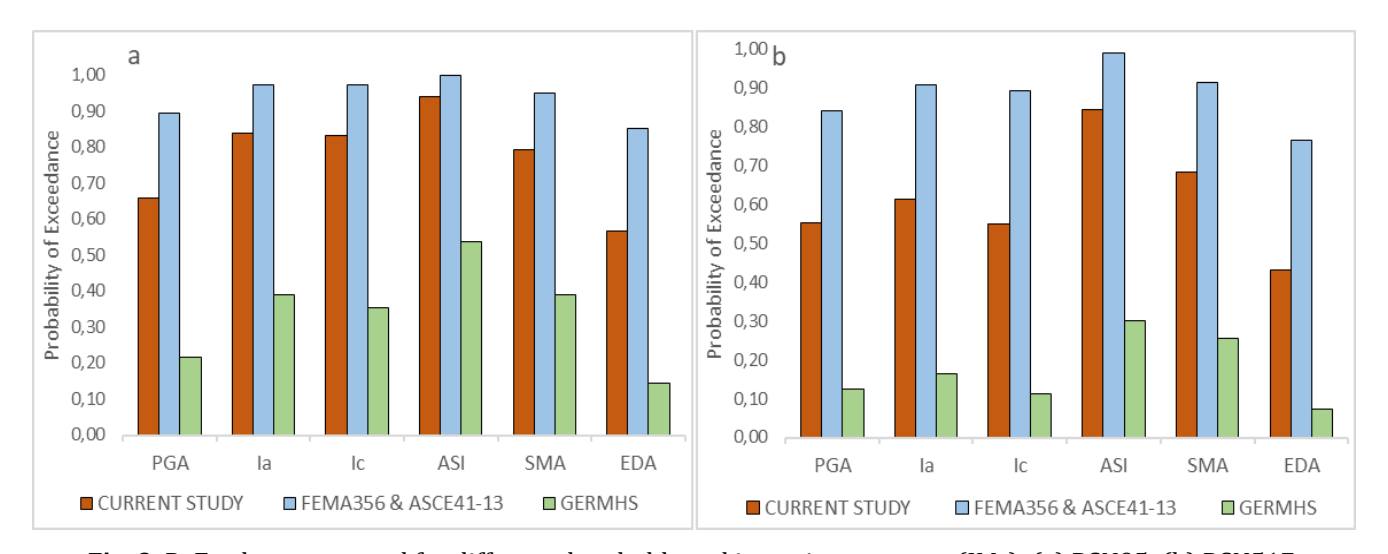


Fig. 9. PoE values computed for different thresholds and intensity measures (IMs): (a) RSN95; (b) RSN517.

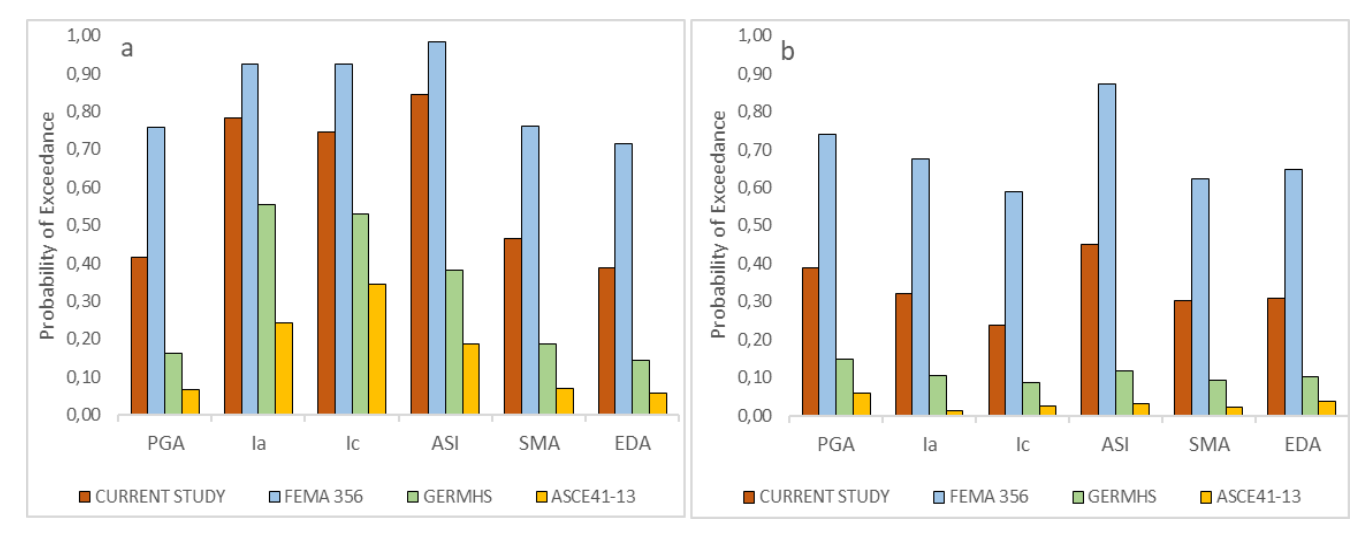


Fig. 10. PoE values computed for different thresholds and intensity measures (IMs): (a) RSN143; (b) RSN1004.

Considering the results of this study as a whole, the damage thresholds used in seismic vulnerability studies have a significant impact on the *PoE* values. Therefore, to carry out a rational and accurate risk assessment, the suitability of the thresholds for the target structure should be thoroughly analyzed, rather than directly using the thresholds presented in the literature.

3. Conclusions

The preservation of historical structures is important for the benefit of future generations. These structures serve as a testament to the cultural characteristics of the period in which they were constructed. In this context, the development of effective decision-making mechanisms based on the reliable assessment of the seismic risk of such structures has become increasingly significant in recent years. The reliability of fragility curves, which are frequently utilized in seismic vulnerability and risk assessment studies, is closely related to the selection of appropriate intensity measures and damage parameters. Moreover, accurately determining the threshold values corresponding to various damage states is critically important for the reliability of these curves.

In this study, the influence of different threshold levels associated with a specific damage state on the seismic vulnerability of a historic masonry aqueduct was examined. For this purpose, a 3D finite element model of the structure was developed, and then response spectrum analyses were conducted. Using the cloud analysis method, the dispersion relationships between the MIDR damage parameter and several *IM* parameters, namely PGA, Ia, Ic, ASI, SMA, and EDA, were obtained. Based on these relationships, fragility curves were developed by adopting MIDR threshold values defined in widely accepted standards such as FEMA 356 (2000), ASCE 41-13 (2013), and GERMHS (2017). Additionally, reference fragility curves were constructed using MIDR values determined via nonlinear static analysis and empirical relationships, and comparative evaluations were carried out through *PoE* values. For instance, at an *EDA IM* value of 0.3 g, the *PoE* value for the "Damage Limitation" damage state in the current study was calculated as 0.468, while the corresponding values based on FEMA 356 (2000), ASCE 41-13 (2013), and GERMHS (2017) were 0.792, 0.792, and 0.088, respectively. In the analysis of the "Heavy Damage" state, for an SMA value of 0.7 g, the PoE values were calculated as 0.541 for the current study, 0.813 for FEMA 356 (2000), 0.244 for GERMHS (2017), and 0.107 for ASCE 41-13 (2013). Similarly, for an ASI value of 0.75 g, the *PoE* in the current study was found to be 0.622, compared to 0.068 for ASCE 41-13 (2013), 0.938 for FEMA 356 (2000), and 0.196 for GERMHS (2017). Such notable differences were also observed for other IM parameters.

These results emphasize that the determination of threshold values plays a critical role in the development of fragility curves, directly affecting their reliability and the accuracy of the seismic risk assessment. Therefore, rather than directly adopting threshold values presented in the literature, it is essential to conduct a detailed evaluation of their suitability for the specific structural characteristics of the target building.

This study demonstrates the importance of threshold values for different damage states and provides a valuable reference for future research on historic masonry aqueducts with different construction characteristics. In future studies, it is essential to establish a sub-classification of historical masonry aqueducts by considering their construction techniques, material properties, geometric configurations, and different modelling assumptions. Following this classification, the derivation of fragility curves for each subclass under both near- and farfault ground motion sets would provide valuable insights. It is anticipated that such a study would yield valuable outcomes, enabling rapid seismic risk assessments of historical aqueducts located in various regions.

Acknowledgements

None declared.

Funding

The author received no financial support for the research, authorship, and/or publication of this manuscript.

Conflict of Interest

The author declared no potential conflicts of interest with respect to the research, authorship, and/or publication of this manuscript.

Author Contributions

The author confirms sole responsibility for all aspects of the study including conception and design, acquisition of data, analysis and interpretation of data, drafting the manuscript, revising it critically for important intellectual content; and gave final approval of the version to be published.

Data Availability

The datasets created and/or analyzed during the current study are not publicly available, but are available from the corresponding author upon reasonable request.

REFERENCES

AFAD (2023). Şubat 2023 Pazarcık–Elbistan Kahramanmaraş (Mw: 7.7 – Mw: 7.6) depremleri raporu. General Directorate of Earthquake and Risk Reduction, Earthquake Department, Ankara, Türkiye. (in Turkish)

Akturk F, Yesilyurt A, Cakir F (2025). Optimal intensity measures for probabilistic seismic demand modeling of single-domed historical masonry buildings. *Engineering Failure Analysis*, 171,109378.

Alpaslan E, Dinç B, Hacıefendioğlu K, Demir G, Köksal O (2017). Modal identification of a reduced-scale masonry arch bridge with experimental measurements and finite element method. *Challenge Journal of Structural Mechanics*, 3(3), 108-115.

Alpaslan E, Karaca Z (2020). Model updating of a reduced-scaled masonry bridge by using response surface method. *Challenge Journal of Structural Mechanics*, 6(1), 41-51.

ANSYS (2022). Engineering Simulation Software. , ANSYS [Online]. Available: https://www.ansys.com

ASCE 41-13 (2013). Seismic rehabilitation of existing buildings. American Society of Civil Engineers, Reston, VA.

Balcan C, Aydın EÖ, Ünsal Ö (2024). Value-based optimization model for cultural route design: Ancient Water Supply Heritage of Istanbul (Türkiye). *Journal of Cultural Heritage*, 70, 97-110.

Cattari S, Calderoni B, Caliò I, Camata G, de Miranda S, Magenes G, Saetta A (2022). Nonlinear modeling of the seismic response of masonry structures: critical review and open issues towards engineering practice. *Bulletin of Earthquake Engineering*, 20(4), 1939-1997.

Cheng G, Zhang Y, Huang J, Liu J, Zhang J (2020, September). Vulnerability analysis of aqueduct structure based on boundary method. IOP Conference Series: Earth and Environmental Science, 567(1), 012036.

Cosgun C, Mangir A (2018). Earthquake performance of collapsed school building under Van-Tabanli (Mw=7.2) earthquake. *Challenge Journal of Structural Mechanics*, 4(4), 159-175.

Çakır F (2021). A simplified method for determining the seismic performance of historical structures: a case of Kaya Çelebi Mosque. Journal of the Faculty of Engineering and Architecture of Gazi University, 36(3), 1643-1656.

Cakir F (2022). Performance-based assessment of long masonry structures. *Challenge Journal of Structural Mechanics*, 8(2), 47-56.

Cakir F, Uckan E, Shen J, Seker BS, Akbas B (2015). Seismic damage evaluation of historical structures during Van earthquake, October 23, 2011. Engineering Failure Analysis, 58, 249-266.

- Cakir F, Uckan E, Shen J, Seker S, Akbas B (2016). Seismic performance evaluation of slender masonry towers: a case study. *The Structural Design of Tall and Special Buildings*, 25(4), 193-212.
- Dogangun A, Sezen H (2012). Seismic vulnerability and preservation of historical masonry monumental structures. *Earthquake and Structures*, 3(1), 83-95.
- Drougkas A (2022). Macro-modelling of orthotropic damage in masonry: Combining micro-mechanics and continuum FE analysis. *Engineering Failure Analysis*, 141, 106704.
- Drucker DC, Prager WJ (1952). Soil mechanics and plastic analysis or limit design. *Quarterly of Applied Mathematics*, 10(2), 157-165.
- Du M, Zhang S, Wang C, She L, Li J, Lu T (2023). Seismic fragility assessment of aqueduct bent structures subjected to mainshock-aftershock sequences. *Engineering Structures*, 292, 116505.
- Du M, Zhang S, Wang C, Li Z, Yao J, Lu T (2024a). Development of the compound intensity measure and seismic performance assessment for aqueduct structures considering fluid-structure interaction. *Ocean Engineering*, 311, 118838.
- Du M, Yang X, Zhang S, Wang C, Guo R, Li Z, Yao J (2024b). Probabilistic seismic performance assessment of aqueduct structures considering different sources of uncertainty. *Structures*, 70, 107750.
- Ercan E, Alver N, Nuhoğlu A (2015). Evaluation of material properties by NDT methods and FEM analysis of a stone masonry arch bridge. *Challenge Journal of Structural Mechanics*, 1(4), 168-172.
- Erdik M, Doyuran V, Akkaş N, Gülkan P (1985). A probabilistic assessment of the seismic hazard in Turkey. *Tectonophysics*, 117(3-4), 295-344.
- Erkek H, Yetkin M (2023). Assessment of the performance of a historic minaret during the Kahramanmaraş earthquakes (Mw 7.7 and Mw 7.6). *Structures*, 58, 105620.
- FEMA 274 (1997). NEHRP commentary on the guidelines for the seismic rehabilitation of buildings. Federal Emergency Management Agency, Washington, DC.
- FEMA 356 (2000). Pre-standard and commentary for the seismic rehabilitation of buildings. Federal Emergency Management Agency, Washington, DC.
- GERMHS (2017). A guideline for earthquake risk management of historical structures in Turkey. General Directorate of Foundations, Ankara, Türkiye.
- Gkournelos PD, Triantafillou TC, Bournas DA (2022). Seismic upgrading of existing masonry structures: A state-of-the-art review. *Soil Dynamics and Earthquake Engineering*, 161, 107428.
- Gonen S, Pulatsu B, Erdogmus E, Karaesmen E, Karaesmen E (2021).

 Quasi-static nonlinear seismic assessment of a fourth century AD
 Roman Aqueduct in Istanbul, Turkey. Heritage, 4(1), 401-421.
- Işık E, Karaşin İB, Demirci A, Büyüksaraç A (2020). Seismic risk priorities of site and mid-rise RC buildings in Turkey. *Challenge Journal of Structural Mechanics*, 6(4), 191-203.
- Kappos AJ, Panagopoulos G, Panagiotopoulos C, Penelis G (2006) A hybrid method for the vulnerability assessment of R/C and URM buildings. *Bulletin of Earthquake Engineering*, 4, 391–413.
- Kocaman İ (2023). The effect of the Kahramanmaraş earthquakes (Mw 7.7 and Mw 7.6) on historical masonry mosques and minarets. Engineering Failure Analysis, 149, 107225.
- Kocaman İ, Mercimek Ö, Gürbüz M, Erbaş Y, Anıl Ö (2024). The effect of Kahramanmaraş earthquakes on historical Malatya Yeni Mosque. Engineering Failure Analysis, 161, 108310.
- Korkmaz M, Ozdemir MA, Kavali E, Cakir F (2018). Performance-based assessment of multi-story unreinforced masonry buildings: The

- case of historical Khatib School in Erzurum, Turkey. *Engineering Failure Analysis*, 94, 195-213.
- Lagomarsino S, Cattari S (2015). PERPETUATE guidelines for seismic performance-based assessment of cultural heritage masonry structures. *Bulletin of Earthquake Engineering*, 13, 13-47.
- Lagomarsino S, Giovinazzi S (2006). Macroseismic and mechanical models for the vulnerability and damage assessment of current buildings. *Bulletin of Earthquake Engineering*, 4, 415–443.
- Lamego P, Lourenço PB, Sousa ML, Marques R (2017). Seismic vulnerability and risk analysis of the old building stock at urban scale: application to a neighbourhood in Lisbon. *Bulletin of Earthquake En*aineering, 15, 2901-2937.
- Liu J, Xu J, Huang L (2025). Seismic vulnerability analysis of aqueducts based on probability density evolution method. *Transportation Research Record*, 2679(6), 203-226.
- Ma Y, Wu Z, Liu Z, Zhang M, Aibaidula M (2022). Seismic fragility analysis of aqueduct structural systems based on G-PCM method. *Sustainability*, 14(20), 13161.
- Ozdemir MA, Kaya ES, Aksar B, Seker B, Cakir F, Uckan E, Akbas B (2017). Seismic vulnerability of masonry Jack arch slabs. *Engineering Failure Analysis*, 77, 146-159.
- Rota M, Penna A, Magenes GJES (2010). A methodology for deriving analytical fragility curves for masonry buildings based on stochastic nonlinear analyses. *Engineering Structures*, 32(5), 1312-1323.
- Vanin F, Zaganelli D, Penna A, Beyer K (2017) Estimates for the stiffness, strength and drift capacity of stone masonry walls based on 123 quasi-static cyclic tests reported in the literature. Bulletin of Earthquake Engineering, 15(12), 5435–5479.
- Vicente R (2008). Estrat'e'gias e Metodologias para Intervençoes ~ de Reabilitacao ~ Urbana—Avaliaç~ ao da Vulnerabilidade e do Risco Sı'smico do Edificado da Baixa de Coimbra. *PhD Thesis*, University of Aveiro, Aveiro, Portugal. (in Portuguese).
- Xu X, Liu X, Jiang L, Ali Khan MY (2021). Dynamic damage mechanism and seismic fragility analysis of an aqueduct structure. *Applied Sciences*, 11(24), 11709.
- Yesilyurt A (2025). Selection of optimum intensity measure parameters for seismic fragility analysis of typical Roman aqueduct. Structures, 71, 108085.
- Yesilyurt A, Akcan SO, Zulfikar A (2021a). Rapid power outage estimation for typical electric power systems in Turkey. *Challenge Journal of Structural Mechanics*, 7(2), 84-92.
- Yesilyurt A, Zulfikar AC, Tuzun C (2021b). Site classes effect on seismic vulnerability evaluation of RC precast industrial buildings. *Earthquakes and Structures*, 21(6), 627-639.
- Yesilyurt A, Akcan SO, Cetindemir O, Zulfikar AC (2024). Probabilistic earthquake risk consideration of existing precast industrial buildings through loss curves. *Geomechanics and Engineering*, 37(6), 565-576.
- Yilmaz MF, Çaglayan BÖ, Özakgül K (2018). Seismic assessment of a curved multi-span simply supported truss steel railway bridge. Challenge Journal of Structural Mechanics, 4(1), 13-17.
- Yücemen MS, Yılmaz Ç (2015). Probabilistic assessment of earthquake insurance premium rates for the Gumusova-Gerede Motorway Section. Challenge Journal of Structural Mechanics, 1(2), 42-47.
- Zhang S, Du M, Wang C, Sun B, She L, Liu W (2022). Fragility analysis of high-span aqueduct structure under near-fault and far-field ground motions. Structures, 46, 681-697.
- Zheng X, Shen Y, Zong X, Su H, Zhao X (2023). Vulnerability analysis of main aftershock sequence of aqueduct based on incremental dynamic analysis method. *Buildings*, 13(6), 1490.